Sulfur flotation performance recognition based on hierarchical classification of local dynamic and static froth features

Yalin Wang[a,**], Bei Sun[a,**], Runqin Zhang[a,**], Quanmin Zhu[b]

[a]*School of Information Science and Engineering, Central South University, China 410083*
[b]*Department of Engineering Design and Mathematics, University of the West of England, Coldharbour Lane, Bristol BS16 1QY, UK*

Abstract

This study proposes a flotation performance recognition system based on a hierarchical classification of froth images using both local dynamic and static features, which includes a series of functions in image extraction, processing and classification. Within the integrated system, to identify the abnormal working condition with poor flotation performance (NB it could be significantly different with the dynamic features of the froth in abnormal working condition), it is functioned firstly with building up local dynamic features of froth image from the information including froth velocity, disorder degree, and burst rate. To enhance the dynamic feature extraction and matching, this system introduces scale-invariant feature transform (SIFT) method to cope with froth motion and the noise induced by dust and illumination. For the performance subdivision under normal working conditions, Bag-of-words (BoW) description is utilized to fill the semantic gap in performance recognition when images are directly described by global image features. Accordingly typical froth status words are extracted to form a froth status glossary so that the froth status words of each patch form the BoW description of an image. A Bayesian probabilistic model is built to establish a froth image classification reference with the BoW description of images as the input. An expectation-maximization (EM) algorithm is used for training the model parameters. Data obtained from a real plant are selected to verify the proposed approach. It is noted that the proposed system can reduce the negative effects of image noise, and has high accuracy in flotation performance recognition.

Keywords: froth flotation; static features; dynamics features; hierarchical classification; performance recognition

1. Introduction

Froth flotation is a widely used mineral separation technology to acquire high-grade concentrates. It has a long process flow which involves complex physical and chemical reactions with various influence factors. Due to reasons like fluctuation of feeding conditions, maloperations and external disturbances, a flotation process exhibits multiple working conditions with different flotation performance. An accurate mathematical model that could comprehensively and precisely describe the dynamics of a froth flotation process, and thus to guide the operation, is costly to obtain. As an alternative, surface froth features, which are closely related to the final concentrate grade and recovery rate, are utilized as the performance indicator in practical production [1].

Performance recognition is crucial and fundamental in the optimal operation of a flotation process. With the development of machine vision and artificial intelligence, digital image processing technology has been widely applied in the classification of froth surface images and recognition of flotation performance [2]. Moolman et al. used digital image analysis and an artificial neural network approach in the classification of froth images [3, 4]. Hargrave et al. studied the prediction of flotation performance through off-line analysis of color, texture, and other visual features of coal and tin froth surface [5]. Singh et al. first divided a froth image into patches. Then extracted the RGB color information of each patch, and used the information in the image classification using a radial basis function neural network [6]. Zhu et al. and He et al. applied the probability density function (PDF) in the description of froth size distribution and studied the reagent dosage predictive control of a copper flotation process [7][8]. The above results indicate the effectiveness of the static froth features, such as color, texture, size, in the classification of froth images and identification of flotation performance. On the other hand, researchers have studied the relationship between dynamic froth features, such as froth stability and velocity, and the concentrate grade as well as the recovery rate. Ventura-Medina et al. verified that froth stability plays an important role in flotation performance. They related changes in the fraction of air overflow to the variations in the performance of a copper flotation process [9]. Barbian et al. used the froth stability column method to quantify froth stability on both laboratory scale and industrial scale [10]. The result indicated that lower air flow rates resulted in better froth stability and improved flotation performance [11]. Morar et al., Barbian et al., and Runge et al. verified that froth stability measurements in combination with froth velocity, and without the use of color, can predict concentrate grade [12][13][14]. They concluded that froth stability is related to the concentration of

*Corresponding author
**These authors contributed equally to this work and should be considered co-first authors.
Email address: bei.sun@csu.edu.cn (Bei Sun)

the attached material within the system, whereas the velocity is related to the concentration of entrained material recovered. Morar chose the burst rate of froth surface lamellae to represent froth stability since each burst event signal is not determined by bubble size or any other froth structural features [15].

As indicated by previous studies, both dynamic features, such as froth stability, and static features, reflect flotation performance from different aspects, and should be taken into consideration together in flotation performance recognition. However, there are few studies used both dynamic and static features in flotation performance recognition[16]. For a more detailed review of the application of machine vision in flotation process monitoring and control, the reader is referred to excellent reviews such as [17, 18, 19] and the references therein.

For sulphur flotation process, due to the high hydrophobicity of sulphur, the addition of chemical reagents is not required. The operations mainly include adjusting of air flow rate and pulp level. It is important to keep the pulp level around optimal to assure that a sufficient part of the valuable froth is collected while abnormalities like turning pulp is avoided. According to expert experience, when pulp overflows, the froth exhibits distinct dynamic features compared with normal working conditions. This is verified in [20, 21, 22] which concluded that the variation of pulp level is reflected by the dynamic froth features including velocity, disorder degree and burst rate.

This study utilized both local dynamic and static froth features to detect the abnormal working condition and evaluate the sulfur flotation performance under normal working conditions. In Section 2, the sulfur flotation process is introduced and analyzed, and a hierarchical flotation performance recognition framework is proposed. In order to obtain the dynamic features of froth and avoid the semantic gap in performance recognition when images are directly described by global image features, the froth images are divided into local patches. Section 3 studies the detection of abnormal working conditions using local dynamic froth features. Three local dynamic features of the froth, including froth velocity, disorder degree, and burst rate, are extracted using the Scale Invariant Feature Transform (SIFT) algorithm. These local dynamic features are then used to detect the abnormal working conditions. Section 4 considers the evaluation of flotation performance under normal working conditions using local static froth features. The local static features such as texture and color are extracted to obtain the 'Bag of Words'(BoW) description. The flotation performance is then recognized using a Bayesian probabilistic model. By comprehensively considering the relationship between flotation performance and local dynamic and static froth features, a hierarchical sulfur flotation performance recognition system is established. In Section 5, the proposed approach is tested through simulation experiments with data collected from a real plant.

2. Problem analysis

In metallurgy plants, sulfur flotation is used to recover valuable sulfur as a secondary product from leaching residues of sulfide minerals. It is conducted by taking advantages of the naturally strong hydrophobicity of sulfide ores. The addition of chemical reagents is not necessary. The operation of sulfur flotation mainly involves the adjusting of pulp level and inlet air flow. As shown in Fig. 1, air is blew into the flotation cell to enable the formation of air bubbles with mineral particles attached. The sulfur concentrate is recovered by collecting the mineralized froth at the overflow of the flotation cell.

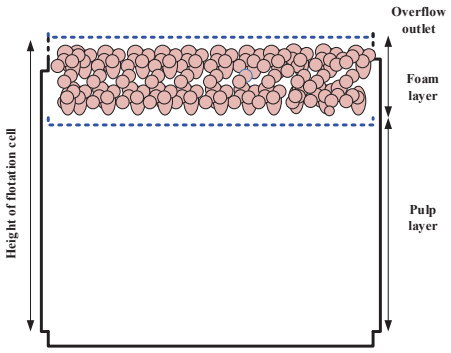

Figure 1: Cross-section diagram of a flotation cell

The thickness of froth layer has a large impact on the concentrate grade. Increasing the thickness of the froth layer can prolong the residence time of the solid particles in the froth layer. It is beneficial to the detachment of gangue, and thus improve the concentrate grade. The height of the flotation cell is fixed, and equals to the sum of the pulp level and thickness of the froth layer. If the pulp level is low, then the froth layer is thick, and vice versa. Therefore, pulp level, which indicates and affects the flotation performance, is a key variable in sulfur flotation.

Pulp level is related to a number of dynamic froth features. When the pulp level is too high, the froth layer is extremely thin. The froth mainly consists of blister and flows fast. This may lead to the spillover of pulp and a low concentrate grade. When the pulp level is too low, the froth layer is excessively thick. The froth becomes sticky and difficult to collapse or burst. This leads to a slow froth overflow, or even non-overflow, resulting in low recovery. Hence, changes in pulp level are directly reflected in the ***dynamic features*** of froth image, including velocity, disorder degree, and burst rate, which reflect flotation performance to a large extent. On the other hand, froth images under different working conditions exhibit different ***static features***, such as the fineness of froth texture, depth of grooves, etc. In addition, the froth color reflects the quantity of minerals carried by the froth.

Therefore, in order to improve the recognition performance, a flotation performance recognition system based on the hierarchical image classification using both local dynamic and static features is proposed (Fig. 1). In order to detect the abnormal working conditions, a SIFT operator is incorporated in a feature matching approach to extract the local dynamic features of sulfur flotation froth. When the process is under normal working conditions, static froth features are utilized in the recognition. The local froth features, such as texture and color, are transformed into codewords which are then described using the

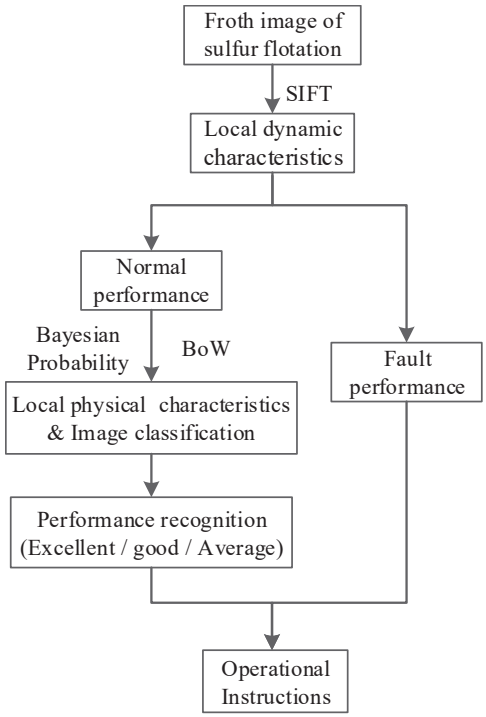

Figure 2: The hierarchical performance recognition system based on both local dynamic and static froth features

BoW model. The Bayesian probabilistic model is introduced to train the model parameters using the expectation-maximization algorithm(EM).

3. Abnormal working condition recognition based on Scale-Invariant Feature Transform

In this section, a feature matching method based on SIFT is devised to extract the local dynamic features of froth image. First, three local dynamic features, i.e., speed, disorder degree, burst rate, and their computing formulas are selected and defined, respectively. Then, the relationship between these features and flotation performance is analyzed using froth images collected from a sulfur flotation plant. These dynamic features are used to detect the abnormal working condition, which laid a foundation for the later 'static features-based' flotation performance subdivision under normal working conditions.

3.1. Key points extraction and matching

SIFT algorithm is a local feature descriptor based on scale space theory[23][24]. The main idea of scale pace theory is to present the original image on different scales and to extract the invariant key points, edge, corner, as well as other features. SIFT is invariant to rotation, scaling, brightness change and affine transformation of image, and holds a certain stability towards angular variation and noise. For two consecutive images to be matched, two vector sets of key points in the two images can be obtained. Then, the vector similarity is calculated to determine whether the two key points match. Implementation of SIFT algorithm is as follows,

- The detection of key points in froth images;
- Accurate positioning of key points;
- Calculating the orientation parameters of key points;
- Generation of parametric statistics and the final description vector of key points.

The effectiveness of SIFT was tested under three typical categories of froth status. In the first category, the moving speed of froth is moderate and the moving direction is stable and uniform. The froth has good surface adhesion and hardly burst. In the second category, froth moves faster with disordered directions and less foam on the surface, resulting in low concentrate grade. In the third category, froth moves in a high speed which resulted in blurry froth surface and poor flotation performance. The matching results are shown in Fig. 2 (the coordinates are pixel coordinates). In Fig. 2 (a), (c), and (e), red line depicts matching result of the key points. The two endpoints of each red line represent the two matched key points. (Because of the large number of matched points, the figure shows only part of the key points). Fig. (b), (d), and (f) show schematic views of the velocity field of each category.

3.2. Local dynamic features extraction based on SIFT

According to the result of section 3.1, froth velocity, disorder degree and burst rate are selected as the dynamic features of froth. The formulae of these dynamic features are given in Eqs. (1) to (7).

Consider two consecutive images, the key points are first extracted. The pixel displacements in the X and Y directions of the key point in unit time are obtained, as well as the velocity of the froth. Take the pixel displacements of two consecutive images in the X direction as x, the pixel displacement in the Y direction as y, the velocity in the horizontal direction as V_x, the velocity in the vertical direction as V_y, the froth velocity as V, and the movement direction as θ. Then if the sampling rate of the cameras in the sulfur flotation plant is D frame images per second, the equations for these variables are as follows,

$$V_x = \sum_D x \tag{1}$$

$$V_y = \sum_D y \tag{2}$$

$$V = \sqrt{V_x^2 + V_y^2} \tag{3}$$

$$\theta = \arctan\frac{V_y}{V_x} \tag{4}$$

The unit of the velocity's magnitude and velocity's direction is pixel/sec (pixel per second) and deg/s (degree per second), respectively. In addition, to describe the disorder degree, express the froth velocity as,

$$V = \bar{V} + V', \tag{5}$$

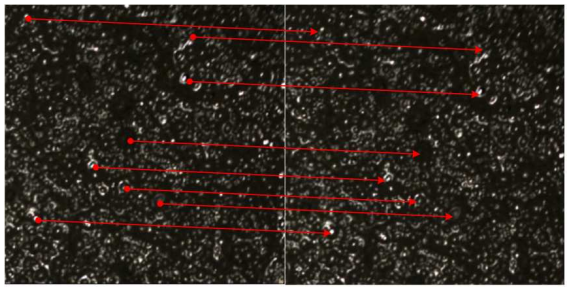

(a) SIFT-based matching results in the first category

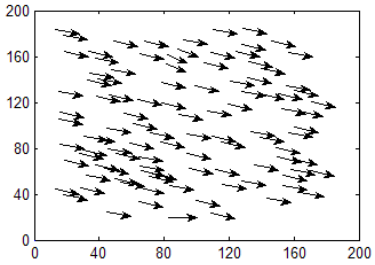

(b) Froth velocity field of the first category

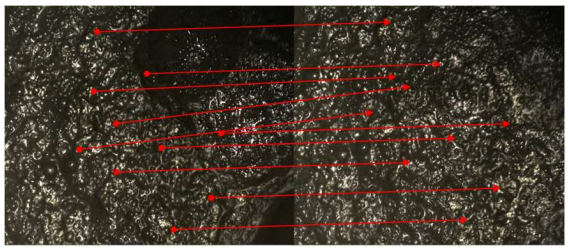

(c) SIFT-based matching results in the second category

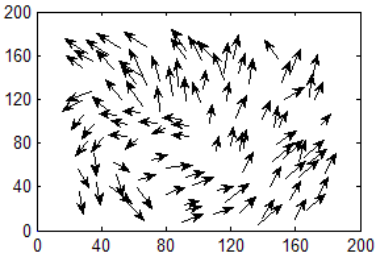

(d) Froth velocity field of the second category

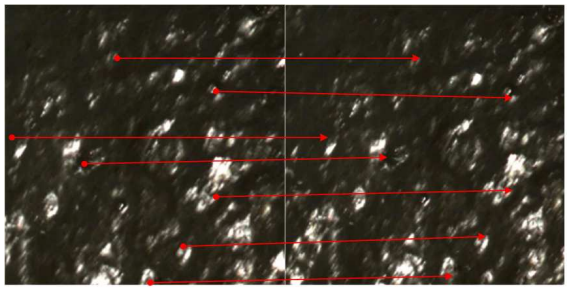

(e) SIFT-based matching results in the third category

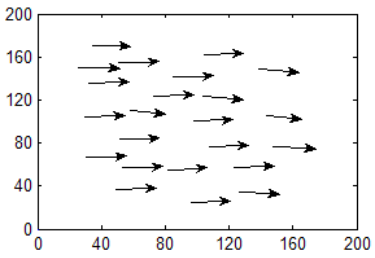

(f) Froth velocity field of the third category

Figure 3: Schematic view of froth velocity field in different categories

where $\bar{V}$ is the average velocity of the froth over a period of time, and V' is the fluctuation of froth velocity. Then, define the following,

$$V_T = \frac{\sqrt{V'^2}}{V}. \quad (6)$$

The average value of V_T over a certain period of time is taken to represent the froth disorder degree. Besides the fluctuation in velocity magnitude, the change in froth velocity direction also reflects the disorder degree of froth movement to some extent. It can be noted from Fig. 2 that, in Fig. 2(d) the change in froth movement direction is more obvious than the change in Fig. 2(b) and (f), which is relatively stable.

Froth burst rate can be measured by the ratio of the total number of key points and the number of matched key points. The greater the ratio, the higher the burst rate:

$$S = \frac{\bar{N}_{sum}}{N_{match}}, \quad (7)$$

where $\bar{N}_{sum}$ is the average number of key points in two adjacent frames of images, and N_{match} is the number of matched key points in two adjacent frames of images.

3.3. Abnormal working condition recognition based on local dynamic features

A flotation process has both normal and abnormal working conditions, and according to the different grades of concentrate, the flotation performance under normal working conditions can be divided into three categories like excellent, good, and general, see Table 1. Froth images representing the four performance categories are shown in Fig. 4.

Table 1: Flotation froth appearance in different performance categories

Category	Froth appearance description
Excellent	Moderate froth size and thickness, moderate velocity magnitude, and stable movement direction
Good	Uneven froth size distribution, easily burst, moderate velocity magnitude, and stable movement direction
General	Blurry froth surface, less concentrate attached, high velocity, stable movement direction
Abnormal	No significant froth on the surface, deep texture, high velocity and disordered movement

Consider a froth image sequence collected from a plant in three different time periods (denoted as A, B, and C), time period A refers to normal performance, while time period B and C refer to abnormal performance. The local dynamic froth features extracted using the SIFT image matching algorithm are shown in Fig. 5. Fig. 5 (a)-(f) show froth velocity and froth velocity direction in time periods A, B and C. Fig. 5 (g) shows the froth burst rate in time periods A, B and C.

As can be seen from Fig. 5, the dynamic features in the three time periods showed great differences. Flotation performance in time period A is normal, in which the velocity magnitude kept in the range of 300-500 pixels/sec and movement direction maintained at a small range of 40-65 deg/s. However, in time period B, the froth velocity magnitude is in the range of 600-700 pixels/sec, which indicates a very high speed. The movement direction maintained at a smaller range of 20-35 deg/s, froth during this period is likely to burst, and this resulted in unsatisfying flotation. In time period C, both froth velocity and velocity direction fluctuate sharply, and froth movement is disordered. This is due to turning pulp, which indicates poor flotation performance and should be avoided.

4. Froth image classification based on the BoW model and Bayesian probabilistic model

Global features extracted from two distinct images may be very similar, resulting in lower accuracy froth image classification and performance recognition. Moreover, when the image is processed as a whole, describing the image using global features is unintelligible. There exists a semantic gap problem in the classification, i.e., the inconsistency between global features and high-level semantic. In addition, due to dust and illumination, the noises in froth images have diverse impacts on different categories of froth images. Hence, to improve the accuracy of image classification and performance recognition, as well as to achieve optimal control of sulfur flotation, local dynamic froth features are extracted and utilized in this study. An image is first divided into patches. The texture and color features of local patches are extracted, and transformed into words of froth status. Then, the BoW description of the images is obtained. The Bayesian probability model is introduced, and EM (Expectation-Maximization) algorithm is used for training model parameters.

4.1. BoW description of froth image

The BoW description of froth images is inspired by the BoW text classification model[25][26]. BoW is a simplified representation model, in which a text (or document) is represented as a bag of keywords and phrase. The grammar and the order of words in the text are ignored. In a document, the occurrence frequency of each key word is a representation of the theme. Similarly, in image classification, the occurrence frequency of each froth status word indicates the theme of an image, i.e., the category an image belongs to.

To start with, K-means clustering method is applied to obtain the froth status glossary,

- Step 1: Select N frames of images from the image library. The selected images should cover as much categories of flotation performance as possible;
- Step 2: Divide each image into $m \times m$ patches with the same pixel size $L_x \times L_y$;
- Step 3: Extract texture features (ASM, ENT, CON, IDM, COR) and relative red component values of each patch of each image to form a 1×6 dimensional feature description vector;

(a) Excellent

(b) Good

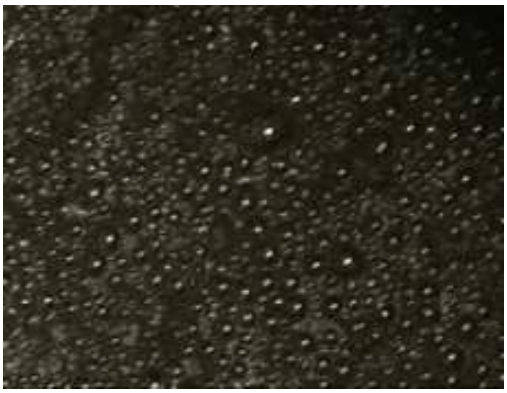

(c) General

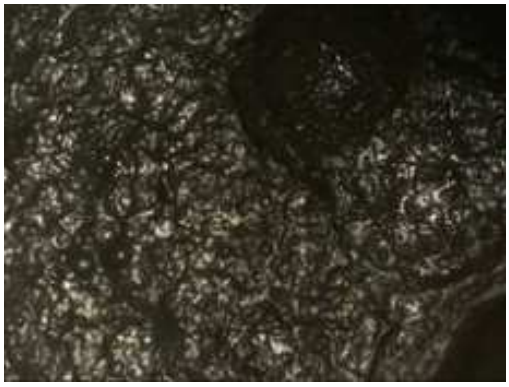

(d) Abnormal

Figure 4: Sulfur flotation froth images under different performance categories

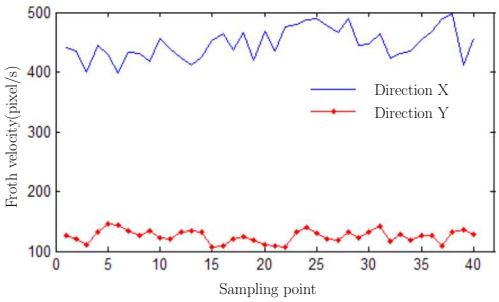

(a) Froth velocity in period A

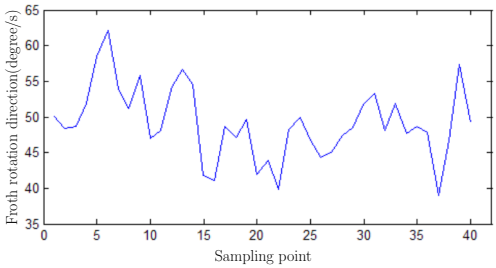

(b) Froth velocity direction in period A

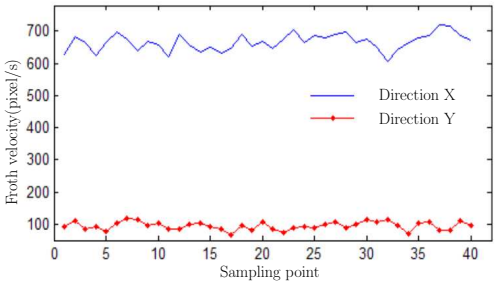

(c) Froth velocity in period B

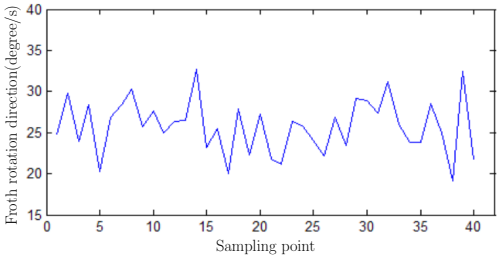

(d) Froth velocity direction in period B

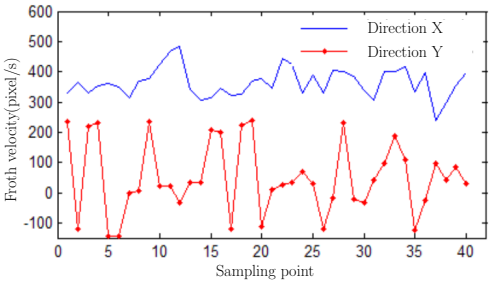

(e) Froth velocity in period B

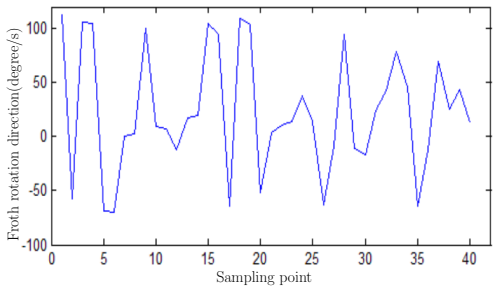

(f) Froth velocity direction in period C

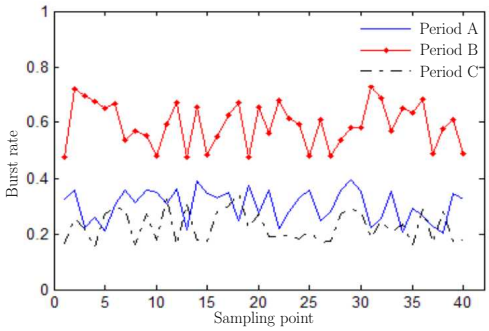

(g) Abnormal

Figure 5: Froth burst rate in periods A, B, and C

- Step 4: Cluster all the feature description vectors using K-means method to obtain D clustering centers, which are the words of froth status. Then, the froth status glossary is obtained.

After the establishment of the froth status glossary, the BoW approach can be adopted to describe the froth image. BoW description of a froth image is a $1 \times D$ dimensional vector, in which each element illustrates the occurrence frequency of corresponding froth status word in the patches. The acquired BoW description of a froth image is shown in Fig. 5. The acquisition steps are given as follows.

- Step 5: As each patch of the under processing image has different local features, repeat steps 1-3 to acquire feature vector description of each patch;
- Step 6: Obtain the similarity between the feature vector of each patch with the words in the froth status glossary by calculating the Euclidean distance. Then, choose the one with the highest similarity as the froth status word of the patch.
- Step 7: Calculate the frequency of each froth status word to obtain the BoW description.

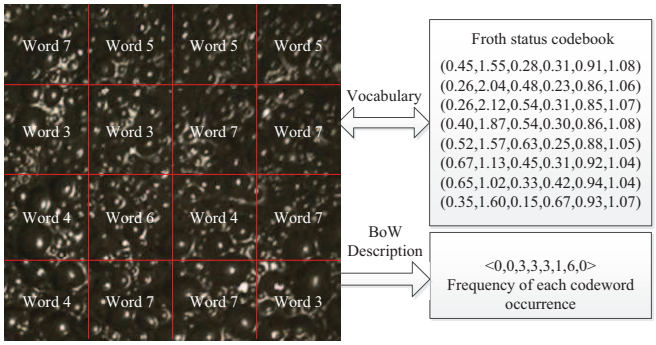

Figure 6: BoW description of froth images

As can be seen from Fig. 6, the BoW of a froth image is obatined as $[0, 0, 3, 3, 3, 1, 6, 0]$. Its high-level semantic meaning could be derived from the BoW description. The BoW description vector is a 1×8 vector, which means there are 8 froth status words in the froth status glossary. In the BoW description vector, 6 means that the 7th froth status word appeared 6 times, which indicates plenty of big froth in the image. Elements with a value of 0 had no corresponding froth status word in the image, which means that the image did not contain blurry or smooth texture regions. This description is similar to human understanding, which from a certain perspective fills the semantic gap.

4.2. Froth image classification based on the Bayesian probabilistic model

The Bayesian theorem derive the probability of an event based on prior probability of conditions related to the event. In sulfur flotation froth image classification, in order to make full use of prior knowledge (prior probability) and sample information, the following assumptions are made.

- One image solely belong to one category $z_k \in \{z_1, \cdots, z_{N_z}\}$, e.g., excellent, good, general.
- Category variables $z_k (k = 1, 2, 3, \cdots, N_z)$ obey the polynomial distribution on all froth image sample sets.
- Froth status words $\omega_j (j = 1, 2, 3, \cdots, N_w)$ obey the polynomial distribution on a certain category z_k.

On the basis of the above three assumptions, define following variables: $p(d)$ represents the occurrence probability of a BoW vector (abstracted from a froth image) in the sample set, $p(\omega_j \mid z_k)$ depicts the occurrence probability of froth status word ω_j when the corresponding category z_k is set, $p(z_k, d)$ stands for the probability distribution of all categories in one image. Thus, the joint probability distribution of the froth status word ω_j and BoW vector d is,

$$p(d_i, \omega_j) = p(d)p(\omega_j \mid d) \tag{8}$$

$$p(\omega_j \mid d) = \sum_{k=1}^{N_z} p(\omega_j \mid z_k)p(z_k \mid d) \tag{9}$$

Thus

$$p(d, \omega) = p(d) \sum_z p(z \mid d)p(\omega \mid z) \tag{10}$$

which can also be formulated as

$$p(d, \omega) = \sum_z p(d)p(d \mid z)p(\omega \mid z). \tag{11}$$

Therefore, for the whole BoW vector set and froth status glossary, the model becomes

$$P(D, W) = \prod_d^D \prod_w^{N_w} p(d) \sum_z p(z \mid d)p(\omega \mid z), \tag{12}$$

where d_i is the ith BoW vector in the sample set, N_w is the number of froth status words, and D is the number of BoW vectors in the sample set. The total number of model parameters is $D \cdot N_z + N_z \cdot N_w$.

Hence, the maximum likelihood parameter optimization problem of the classification model based on the Bayesian probabilistic model can be formulated as

$$\begin{aligned} \max \quad & \log P(D, W) \\ \text{st.} \quad & \sum_z p(z \mid d) = 1 \\ & \sum_z p(\omega \mid z) = 1 \\ & \sum_z p(d) = 1. \end{aligned} \tag{13}$$

Since the model contains unobservable parameter z, the Expectation-Maximization algorithm (EM) [27] is applied in the identification. The steps are described below.

- Initializing the model parameters $p(\omega \mid z)$ and $p(\omega \mid d)$ according to the experts' experience and knowledge.
- Step 'E': Calculate $p(z \mid \omega, d)$.

$$p(z \mid \omega, d) = \frac{p(\omega \mid z, d)}{p(\omega, d)} = \frac{p(\omega \mid z)p(z \mid d)}{\sum_z p(\omega \mid z)p(z \mid d)} \tag{14}$$

  Here, $p(z \mid \omega, d)$ is the category distribution of froth status words in a specific given froth image.

- Step 'M': Calculate the derivations of the parameters, the maximum likelihood condition is met when the derivatives are equal to 0. Therefore,

$$p(d) = \frac{\sum_\omega \sum_z n(d, \omega)p(z \mid \omega, d)}{\sum_d \sum_\omega \sum_z n(d, \omega)p(z \mid \omega, d)} = \frac{n(d)}{\sum_n n(d)}, \tag{15}$$

$$p(\omega \mid z) = \frac{\sum_d n(d, \omega)p(z \mid \omega, d)}{\sum_\omega \sum_d n(d, \omega)p(z \mid \omega, d)}, \tag{16}$$

$$p(z \mid d) = \frac{\sum_\omega n(d, \omega)p(z \mid \omega, d)}{\sum_z \sum_\omega n(d, \omega)p(z \mid \omega, d)} = \frac{\sum_\omega n(d, \omega)p(z \mid \omega, d)}{n(d)}, \tag{17}$$

where $n(d, \omega)$ indicates the times that froth status word ω appears in froth image d. Step 'E' and step 'M' conduct iteratively until convergence. The resulted model parameters $p(\omega \mid z)$ and $p(z \mid d)$ can then be used to derive the category of the froth image.

4.3. Experimental verification and analysis

In Section 3, by using the dynamic feature extraction based on the SIFT feature matching method described, abnormal working condition can be identified when the dynamic features exceed a predefined threshold. This section deals with the classification of flotation performance under normal working conditions. The number of flotation performance categories is set as $N_z = 3$. We collected 300 froth images cover all the three categories (excellent, good, general) from a plant, 150 images for model training and the rest 150 images for testing. Before conducting the experiment, the images were labelled manually according to experts' experience. The labelling result was then used as a reference to evaluate the image classification result.

In the simulation, the size of froth status glossary is assumed to be 20. The performance of the proposed image classification approach is illustrated in Fig. 7 and Table 2. Fig. 8 and Fig. 9 illustrate the impact of the size of froth status glossary and the number of patches in an image on the classification results.

The simulation result indicates a high classification accuracy. In addition, the size of froth status glossary and the number of patches in an image have an impact on the classification result. Increase the size of glossary would improve the classification accuracy. However, the flotation froth image obtained has a low gray level and the contrast between images in different categories are not obvious. And beyond certain limits, increasing the size of the glossary can not result in a higher classification accuracy. So a large froth status glossary is not advised. Similar phenomena was found in the relation between classification accuracy and the number of patches in an image.

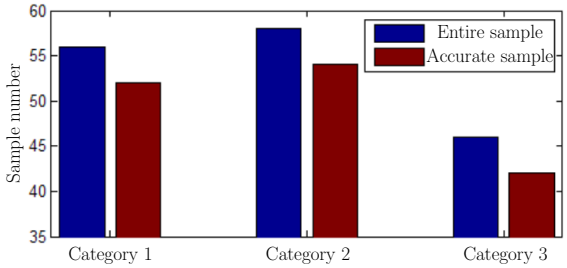

Figure 7: Image classification result based on Bayesian probabilistic model using local static features (N_z=3, the size of froth status glossary N_w=20)

Table 2: Statistics of froth image classification result (N_z=3, the size of froth status glossary N_w=20)

Numbers	Excellent	Good	General
Samples	56	58	46
Accuracy	52	54	42
Accuracy rate	92.8%	93.1%	91.3%

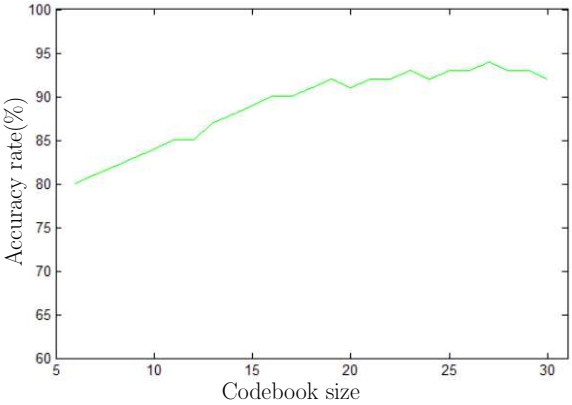

Figure 8: Influence of codebook size on classification accuracy

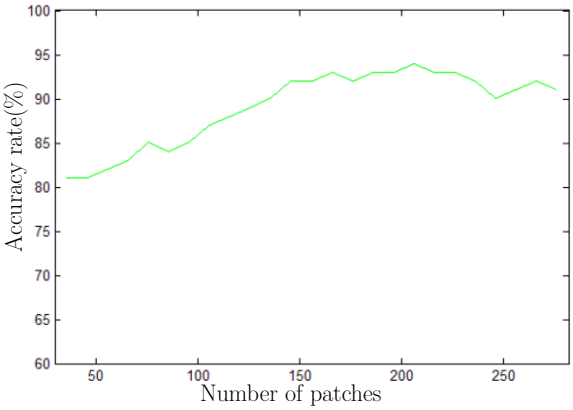

Figure 9: Influence of number of patches on classification accuracy

5. Results and Discussion

5.1. Recognition of abnormal working condition

Fig. 10 shows the distribution of froth image samples, where the axes are the parameters of two local dynamic features (velocity and disorder degree). Statistical results of the normal and abnormal working conditions based on classification of froth velocity and disorder degree are shown in Table 3. The classification and recognition system showed high accuracy for normal working condition recognition, up to 96.5%. The accuracy for abnormal working condition recognition is 86.7%.

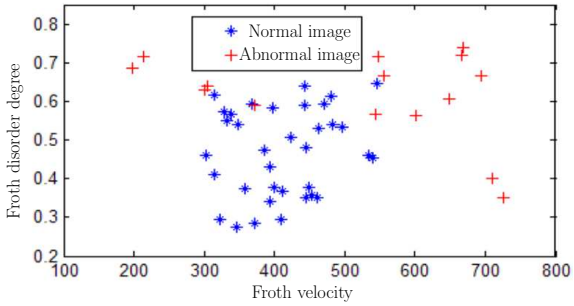

Figure 10: Feature distribution under normal and abnormal working conditions

Table 3: Classification performance using velocity and disorder degree

Category	Normal	Abnormal
Manual classification	57	15
System classification	59	13
Errors	2	2
Accuracy	96.5%	86.7%

5.2. Hierarchical classification system

Figs. 11 and 12 show the classification result with a combination of local physical and dynamic features. The static features, such as texture and color features, are normalized and converted into one parameter, which is denoted as mean absolute of texture. Fig. 11 gives the distribution result of manual classification of froth image samples, and Fig. 12 shows the distribution result of the proposed classification system. Statistical result of the hierarchical classification system based on dynamic and static characteristics are shown in Table 4, where A, B, C, and D correspond to four categories of froth performance (excellent, good, general, and abnormal, respectively). The result indicated that the proposed hierarchical classification based on local dynamic and static features could accurately identify the four types of froth.

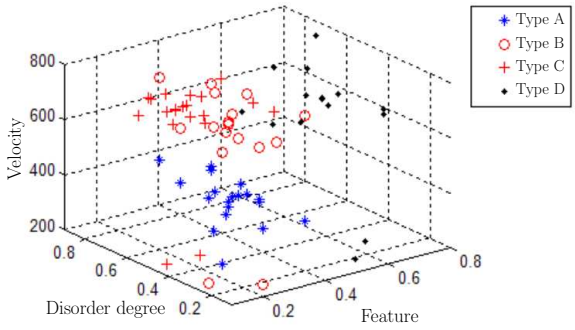

Figure 11: Manual classification result

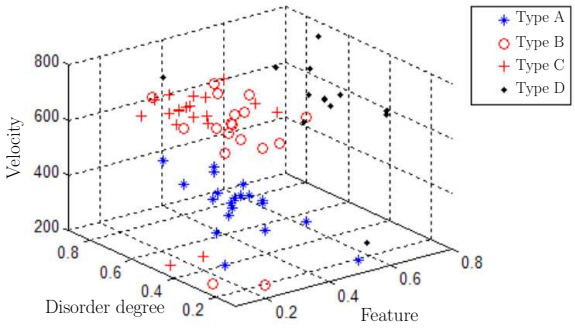

Figure 12: Classification result using the proposed method

Table 4: Statistical results of the proposed classification system

Category	A	B	C	D
Manual classification	19	18	20	15
System classification	21	18	22	13
Errors	2	1	3	2
Accuracy	89.5%	94.4%	85.0%	86.7%

6. Conclusions

A sulfur flotation performance recognition system based on hierarchical classification was developed in this paper. Since froth shows largely different dynamic characteristics under normal and abnormal working conditions in sulfur flotation, both local dynamic and static features were utilized to reduce the limitations introduced by only using static froth features in flotation performance recognition. The experimental results indicate that the abnormal and normal working conditions can be effectively identified with high recognition accuracy. Therefore, this system shows prospect for applications in sulfur flotation plants, and could be tailored and applied in other flotation processes.

The effectiveness of this method could be explained from the perspective of information. In the operation of industrial processes, operators usually encounter the the 'information asymmetry' situation in which the control variables are adjusted with limited information compared with the complex system dynamics and it is thus hard to achieve global optimal[28]. By utilize both local dynamic and static froth features, the 'information asymmetry' situation in sulfur flotation process is lifted. The result in this paper encouraged the development of more advanced flotation performance recognition algorithms which could process more froth features, especially in the context of fiercer competition and the global upgrading of industrial automation system from Industry 3.0 to Industry 4.0.

References

[1] C. Aldrich, D. Moolman, S.-J. Bunkell, M. Harris, D. Theron, Relationship between surface froth features and process conditions in the batch flotation of a sulphide ore, Minerals Engineering 10 (1997) 1207–1218.

[2] J. Bouchard, A. Desbiens, R. del Villar, E. Nunez, Column flotation simulation and control: An overview, Minerals Engineering 22 (2009) 519–529.

[3] D. Moolman, C. Aldrich, J. Van Deventer, D. Bradshaw, The interpretation of flotation froth surfaces by using digital image analysis and neural networks, Chemical Engineering Science 50 (1995) 3501–3513.

[4] D. Moolman, C. Aldrich, G. Schmitz, J. Van Deventer, The interrelationship between surface froth characteristics and industrial flotation performance, Minerals Engineering 9 (1996) 837–854.

[5] J. Hargrave, N. Miles, S. Hall, The use of grey level measurement in predicting coal flotation performance, Minerals Engineering 9 (1996) 667–674.

[6] V. Singh, S. M. Rao, Application of image processing and radial basis neural network techniques for ore sorting and ore classification, Minerals Engineering 18 (2005) 1412–1420.

[7] J. Zhu, W. Gui, C. Yang, H. Xu, X. Wang, Probability density function of bubble size based reagent dosage predictive control for copper roughing flotation, Control Engineering Practice 29 (2014) 1–12.

[8] M. He, C. Yang, X. Wang, W. Gui, L. Wei, Nonparametric density estimation of froth colour texture distribution for monitoring sulphur flotation process, Minerals Engineering 53 (2013) 203–212.

[9] E. Ventura-Medina, N. Barbian, J. Cilliers, Froth stability and flotation performance, in: Proceedings of XXII International Mineral Processing Congress, Cape Town, South Africa, pp. 937–945.

[10] N. Barbian, E. Ventura-Medina, J. Cilliers, Dynamic froth stability in froth flotation, Minerals Engineering 16 (2003) 1111–1116.

[11] N. Barbian, K. Hadler, E. Ventura-Medina, J. Cilliers, The froth stability column: linking froth stability and flotation performance, Minerals Engineering 18 (2005) 317–324.

[12] S. Morar, D. Hatfield, N. Barbian, D. Bradshaw, J. Cilliers, B. Triffett, A comparison of flotation froth stability measurements and their use in the prediction of concentrate grade, in: Proceedings of the XXIII International Minerals Processing Congress, pp. 739–744.

[13] N. Barbian, J. J. Cilliers, S. H. Morar, D. J. Bradshaw, Froth imaging, air recovery and bubble loading to describe flotation bank performance, International Journal of Mineral Processing 84 (2007) 81–88.

[14] K. Runge, J. McMaster, M. Wortley, D. La Rosa, O. Guyot, A correlation between visiofroth^{tm} measurements and the performance of a flotation cell, in: Ninth Mill Operators Conference, pp. 19–21.

[15] S. H. Morar, D. J. Bradshaw, M. C. Harris, The use of the froth surface lamellae burst rate as a flotation froth stability measurement, Minerals Engineering 36 (2012) 152–159.

[16] Y. Fu, C. Aldrich, Flotation froth image analysis by use of a dynamic feature extraction algorithm, IFAC-PapersOnLine 49 (2016) 84–89.

[17] C. Aldrich, C. Marais, B. Shean, J. Cilliers, Online monitoring and control of froth flotation systems with machine vision: A review, International Journal of Mineral Processing 96 (2010) 1–13.

[18] B. Shean, J. Cilliers, A review of froth flotation control, International Journal of Mineral Processing 100 (2011) 57–71.

[19] I. Jovanović, I. Miljanović, Contemporary advanced control techniques for flotation plants with mechanical flotation cells–a review, Minerals Engineering 70 (2015) 228–249.

[20] T. Subrahmanyam, E. Forssberg, Froth stability, particle entrainment and drainage in flotationła review, International Journal of Mineral Processing 23 (1988) 33–53.

[21] F. Núñez, A. Cipriano, Visual information model based predictor for froth speed control in flotation process, Minerals Engineering 22 (2009) 366–371.

[22] S. Farrokhpay, The significance of froth stability in mineral flotationła review, Advances in colloid and interface science 166 (2011) 1–7.

[23] J. S. Beis, D. G. Lowe, Shape indexing using approximate nearest-neighbour search in high-dimensional spaces, in: Computer Vision and Pattern Recognition, 1997. Proceedings., 1997 IEEE Computer Society Conference on, IEEE, pp. 1000–1006.

[24] D. G. Lowe, Distinctive image features from scale-invariant keypoints, International journal of computer vision 60 (2004) 91–110.

[25] T. Hofmann, Probabilistic latent semantic indexing, in: Proceedings of the 22nd annual international ACM SIGIR conference on Research and development in information retrieval, ACM, pp. 50–57.

[26] D. Filliat, A visual bag of words method for interactive qualitative localization and mapping, in: Proceedings 2007 IEEE International Conference on Robotics and Automation, IEEE, pp. 3921–3926.

[27] A. P. Dempster, N. M. Laird, D. B. Rubin, Maximum likelihood from incomplete data via the em algorithm, Journal of the royal statistical society. Series B (methodological) (1977) 1–38.

[28] B. Sun, S.-L. Jamsa-Jounela, Y. Todorov, L. E. Olivier, I. K. Craig, Perspective for equipment automation in process industries, in: IFAC Control Conference Africa 2017, IFAC, pp. 73–78.